



NUMERICAL INVESTIGATION OF A 5 kW POROUS MEDIUM BURNER WITH AN INTEGRATED HEAT EXCHANGER

Tanju ERGEN*, Onur TUNÇER**, A. Cihat BAYTAŞ***

İstanbul Technical University Faculty of Aeronautics and Astronautics Department of Aeronautical Engineering
Maslak, İstanbul 34469, *ergent@itu.edu.tr, **baytas@itu.edu.tr, ***tuncero@itu.edu.tr

(Geliş Tarihi: 03.11.2014, Kabul Tarihi: 18.05.2016)

Abstract: It is most important that a fuel be burnt in a way with least possible pollution to the environment. In this regard every day new legislation is passed restricting pollutant gas emission. A second important issue is to obtain high-density thermal energy via enhanced volumetric heat release. Porous media combustion offers solutions that address both these issues. In this study, we performed several numerical analyses of a symmetrical two-dimensional problem to investigate combustion within a 5 kW porous burner and thermal efficacy of our design. Solution domain consists of four sub-domains, two porous regions in tandem (first with low porosity and second with high porosity), a water tank with constant flow rate and a solid wall in between those. Methane-air is used as reactant mixture for combustion with different excess air ratios and as a parametric study, various water flow velocities are tested for each excess air ratio. Navier-Stokes, energy (thermal equilibrium model) and species transport equations are solved in two-dimensional symmetrical model. A two-step global methane oxidation mechanism is utilized. Velocities, temperature distributions in both combustion zone and water tank, temperature distribution in the axial direction at the centerline of the combustion zone and heat transfer from combustion zone to water are presented.

Keywords: Porous media, combustion, conjugate heat transfer.

BİR ISI DEĞİŞTİRİCİSİ İLE TÜMLEŞTİRİLMİŞ 5 kW GÜCÜNDE BİR GÖZENEKLI ORTAM YAKICISININ SAYISAL İNCELENMESİ

Özet: Bir yakıtın havayı en az kirletecek şekilde yanması oldukça önemlidir. Her gün bu konu ile ilgili kirletici gaz salımlarını kısıtlayan yeni yasal düzenlemeler yürürlüğe girmektedir. İkinci bir önemli konu da yüksek yoğunlukta hacimsel ısı açığa çıkışını elde etmektir. Gözenekli ortamda yanma bu iki önemli konuda çözüm üretebilmektedir. Bu çalışmada, çeşitli sayısal analizler yapılarak ısı verimliliği ve yanma, 5kW'lık gözenekli ortamda simetrik ve iki boyutlu bir problem şeklinde incelenmiştir. Çözüm alanı dört adet alt-alandan oluşmaktadır; iki art arda gözenekli ortam (ilki düşük poroziteli, ikincisi yüksek poroziteli), sabit akış hızına sahip bir su tankı ve katı duvar. Yanmada tepkimeye girenler olarak metan-hava karışımı değişik fazla hava katsayılarında kullanılmıştır ve yakıcı tasarımının en iyilenmesi amacıyla çeşitli su akış debileri her bir eşdeğerlik oranı için test edilmiştir. Navier-Stokes, enerji (ısı denge modeli) ve tür denklemleri iki boyutlu simetrik modelimiz için çözülmüştür. Metanın oksidasyonunda iki-adımlı global bir mekanizma kullanılmıştır. Hız ve sıcaklık dağılımları hem yanma bölgesinde hem su tankında, yanma bölgesinin ortasında eksenel yönde sıcaklık dağılımı ve yanma bölgesinden su tankına olan ısı geçişi gösterilmiştir.

Anahtar Kelimeler: Gözenekli ortam, yanma, eşlenik ısı geçişi.

NOMENCLATURE

C_p	Specific heat capacity, J/kg.K
d_m	Equivalent pore diameter, m
D	Diffusion coefficient, m ² /s
E	Activation energy, J
EAC	Excess air coefficient
Δh	Enthalpy change, J/kg
k	Thermal conductivity, W/m.K
K	Permeability of porous region, m ²
S_L	Laminar flame speed, m/s
p	Pressure, Pa
R_o	Gas constant, J/mol.K
T	Temperature, K
V	Volume, m ³

Greek Symbols

λ	Binary parameter
μ	Dynamic viscosity, N.s/m ²
ρ	Density, kg/m ³
ε	Porosity

Subscripts

eff	Effective
g	Gas
f	Fluid
s	Solid
w	Water

INTRODUCTION

Combustion in porous media provides a wider power range with high power density and ultra-low emissions of CO and NO_x. Note that environmental restrictions are becoming more

stringent every day. Thus interest in porous media combustion is increasing. Porous media combustors have a wide range of applications. They are used from industrial scale furnaces to mobile heaters in vehicles. They are used to heat greenhouses and airport hangars during the wintertime; furthermore they are used as burners in diesel engines and even gas turbines. Trimis outlines many different fields of application of the porous media combustion technology in his study (2000). Fundamentals of a porous burner depend on a heat resistant and high thermal conductivity inert porous foam material. Porous medium itself acts as a flame holder, thermal energy is thus harvested safely and conveniently. In order the fuel to burn efficiently and flame to be held within the porous medium the porosity and permittivity of the porous medium should be adjusted very well. For the flame to propagate within the porous medium freely Peclet number should have a value above 65. The primary criteria of sustaining combustion in porous media depend on its critical pore size. If the size of the pores is smaller than this critical value, flame is quenched since conduction dominates heat release due to combustion. The Critical pore size can be determined by a modified Peclet number, which was determined experimentally by Babkin et al. (1991). A porous burner is split into two zones: the first region where the reactants are premixed at a molecular level to small pore size and the second region, where combustion takes place. Flame is stabilized at the interface.

$$Pe = \frac{S_L d_m c_p \rho}{k} \quad (1)$$

Most of the investigations for porous media combustion use a one-dimensional approach. Barra and Ellzey (2004) performed a computational study for improving a porous burner using methane air mixture. The maximum temperature was approximately 1600°C in this porous burner. They used thermal equilibrium model for the porous region. They try to determine the porosity permeability of their porous region to obtain efficient combustion. Brenner et al. (2000) designed a porous burner using methane/air mixture. Their porous reactor supplies heat to a heat exchanger. Yu et al. (2013) designed a porous burner using ceramic and metal fibers. They designed also a heat exchanger and investigated the performance and efficacy of the system. In addition, commonly used porous-media burner types were experimentally studied to investigate their emission characteristics for various load conditions (Yu et al., 2013). Ata (2010) constructed an experimental setup using a circular cylindrical porous radiant burner. He measured the temperature distribution within the combustion chamber and also reported emission values. A numerical study had been conducted for a saturated porous square cavity using thermal non-equilibrium model by Baytas and Pop (2002). They demonstrate the effect of thermal non-equilibrium model on both solid and fluid temperature distributions. Emonts (1999) also investigated a 12 kW power porous medium burner. This experimental study was aimed at reducing pollutant emissions and focuses on the emission indices of CO and NO_x. They report velocity distributions and combustion efficiency of porous burner for different fuel/air mixing and different inlet velocities. Smucker and Ellzey (2004) conducted an experimental and computational study on a

two-section porous burner operated on propane-air and methane-air mixtures. They obtained velocity distributions and efficiency of porous burner for different fuel/air mixing and different inlet velocities. Another two-section porous media study that investigates the performance of porous burners used for LPG domestic cooking stoves was conducted by Pantangi et al. (2011). In these two-section porous burners, pore size of the first section is chosen to be smaller than critical pore size dimension. Therefore, the only purpose of existence of this section is to pre-heat the fuel-air mixture before burning. Takeno, Sato and Hase (1981) were the first researchers came up with the idea to use porous media in the combustion area for providing pre-heating of fuel-air mixture prior to combustion.

In more recent studies, Henriquez-Vargas et al. (2015) investigate lean combustibility limits of ethanol/air mixture by computational simulations using two different porous media, alumina foam and packed bed of alumina spheres in their study. Another experimental study was performed recently by Iral and Amell (2015) in two-layer porous media. Other than temperature distribution and emission levels, radiation efficiency and pressure drop across the porous materials was measured in their experiment. And Shin et al (2014), conducted a comprehensive numerical study comparing freely propagating premixed flames and the premixed flames with a porous media for various inlet velocities. They used detailed chemistry for combustion so they were able to investigate pollutant formation as well as flame structure and stabilization characteristics.

In the present study, we perform a numerical analysis of a two-dimensional problem arising from combustion within a porous burner with an integrated heat exchanger. The physical domain consists of two components, porous and water tanks zones. Two-dimensional Navier–Stokes equations, thermal equilibrium energy equations for porous burner and water region are solved using finite volume methods. We investigate the porous burner and efficacy of the overall system. The permeability and porosity of porous region were determined in order to be able to hold the flame properly. Fuel flow rate corresponds to a thermal power of 5 kW based on the lower heating value of the fuel.

MATHEMATICAL MODELLING

Consider the combustion in a two-dimensional porous burner with heat-conducting solid walls of finite thickness d_1 and adjacent water tanks. A schematic geometry of the problem under consideration is provided in Fig. 1, where x and y are the Cartesian coordinates and b is the wall height. It is also assumed that all the walls of the water tanks are adiabatic. Combustion chamber consists of two different porous regions. First region's height is 50 mm and it has low porosity ($\epsilon=0.4$) to only assure pre-heating of the reactant mixture and the second region's height is $b_2=50$ mm has pore diameter larger than critical pore size ($\epsilon=0.87$ porosity) to allow combustion. Combustion zone has a 10 mm wall (steel) thickness and two water tanks, $t_1=40$ mm width, $b_1=100$ mm height with inside panels to control water flow, are attached to the combustion zone from both sides as shown in Fig.1. Fluid flow is assumed to be incompressible, two-

dimensional and axisymmetric. Porous media is homogenous, isotropic and inert with negligible catalytic effects. The fluid within the porous medium saturates the solid matrix and both are assumed to be in thermal equilibrium. The governing equations for the flow, species concentrations, and temperature during forced convection in a porous burner are solved numerically. Simplified combustion models are proven to be applicable for porous burners, Moraga et al (2008), model their methane/air combustion with single-step chemical reaction. In this study combustion is modeled using a two-step global methane-air oxidation mechanism, which consists of two reactions and six chemical species. Two different porous regions can be combined into a single set of equations from the continuation of the physical quantities by introducing the following binary parameter in Eq. 2.

$$\lambda = \begin{cases} 0 & \text{in the water region} \\ 1 & \text{in the porous region} \end{cases} \quad (2)$$

Species concentration balance equation is provided in Eq. 3.

$$\nabla \cdot \{ [\varepsilon\lambda + (1-\lambda)] \rho \mathbf{V} \} = 0 \quad (3)$$

Similarly the momentum balance equation is given in Eq. 4.

$$\rho \left\{ \frac{\lambda}{\varepsilon} + (1-\lambda) \right\} \{ \mathbf{V} \cdot \nabla \mathbf{V} \} = -[\varepsilon\lambda + (1-\lambda)] \nabla p + \nabla \cdot (\mu \nabla \mathbf{V}) - (\lambda) \frac{\varepsilon \mathbf{V}}{K} \quad (4)$$

Table 1. Solid and fluid properties

	Water	Air	Methane	SiC
Density at 30°C (kg / m ³)	995.7	1.166	0.65	3200
Dynamic Viscosity (x 10 ⁻⁴ Pa.s)	7.98	0.174	2.1	-
Specific Heat at 30°C (kJ / kg.K)	4.178	1.007	2.22	0.75
Thermal Conductivity at 30°C (W / m.K)	0.58	0.0264	0.035	120

Boundary conditions for the flow domain are provided in Equations 12 through 15.

$$x = 0 \quad 0 < y < b_1 \quad q'' = 0 \quad u = v = 0 \quad (12)$$

$$y = \begin{cases} b_2 + b_3 \\ b \end{cases} \quad 0 < x < t_1 \quad q'' = 0 \quad u = v = 0 \quad (13)$$

$$x = t_1 \quad 0 < y < b_2 + b_3 \quad q'' = 0 \quad u = v = 0 \quad (14)$$

$$y = b \quad t_1 < x < t_1 + t_2 \quad \frac{\partial T}{\partial y} = \frac{\partial u}{\partial y} = \frac{\partial v}{\partial y} = u = 0 \quad (15)$$

Inlet water temperature to heat exchanger is 298 K. Fuel and air is entering with 1 atm and the channel is open to atmosphere.

NUMERICAL SOLUTION PROCEDURE

The numerical method used for discretizing the system of equations for the axisymmetric cartesian composite fluid and porous system is the finite control volume method as outlined in Patankar (1980). The combined continuity, momentum, energy and concentration equations (Equations 1 through 7) are solved numerically using the SIMPLE algorithm by Patankar (1980). The grid layout was arranged by utilizing a non-staggered (collocated) grid procedure, while a power law differencing scheme was adopted for the convection-diffusion terms. The control volume formulation utilized in the SIMPLE algorithm ensures the continuity of the convective and diffusive fluxes as well as the overall

Mass balance equation for fuel vapor is provided in Eq. 5.

$$\rho (\mathbf{V} \cdot \nabla c) = \rho D \nabla^2 c - \rho f c e^{-E/R_0 T_0} \quad (5)$$

Energy balance equation is provided for water and porous regions in Eq. 6 and Eq. 7 respectively.

$$\rho C_p (\mathbf{V} \cdot \nabla T) = k_w \nabla^2 T \quad (6)$$

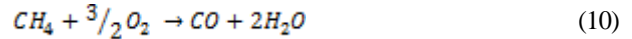
$$(\rho C)_{\text{eff}} + (\rho C)_f \mathbf{V} \cdot \nabla T = \nabla (k_{\text{eff}} \nabla T) - \varepsilon (\rho C)_{\text{eff}} \Delta h f e^{-\Delta E/R_0 T} \quad (7)$$

$$(\rho C)_{\text{eff}} = (1 - \varepsilon)(\rho C)_s + \varepsilon(\rho C)_f \quad (8)$$

$$k_{\text{eff}} = (1 - \varepsilon)k_s + \varepsilon k_f \quad (9)$$

Here, \mathbf{V} is the intrinsic average velocity vector including components. The component of u is in x direction and v is in the y direction. P is pressure, K the permeability of porous material, μ the dynamic viscosity and ρ the density of mixture. E is the activation energy, Δh combustion enthalpy, R universal gas constant.

Two step methane oxidation mechanism is provided in Eq. 10 and Eq. 11. Note that the second reaction is treated as reversible and accounts for the dissociation of carbon dioxide.



momentum, energy and concentration. The harmonic mean formulation adopted at the interface or the diffusion coefficients between two control volumes can deal with abrupt changes without requiring an excessively fine grid at the porous/fluid layer interface.

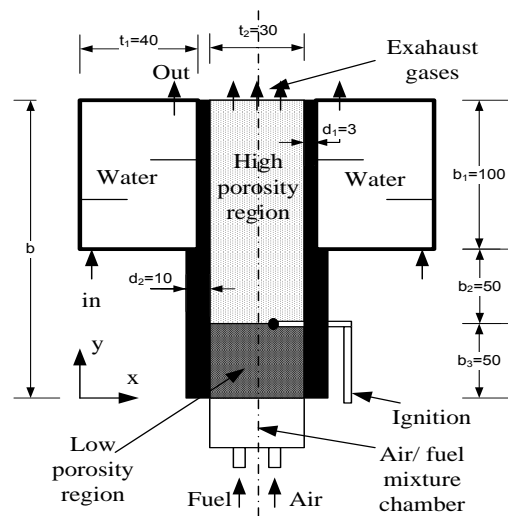


Figure 1. A schematic view of the porous media burner with integrated heat exchanger (all dimensions are in mm)

The mesh system for the entire domain is a non-uniform structured grid and the total number of cells in the region of the water is 100×85 and porous burner region for 200×50 as a trade-off between numerical accuracy, stability and computational time. The resulting system of algebraic equations is solved through the tri-diagonal matrix algorithm (TDMA). Convergence was assured when the maximum errors became less than 10^{-6} . In order to activate the reaction mechanism, an ignition kernel is provided at the interface between high and low porosity media as an initial condition. A zero gradient pressure boundary condition at burner outlet is imposed.

RESULTS AND DISCUSSION

Computations were carried out in order to determine the parametric effect of porosity, inlet gas velocity and excess air coefficient changes on the fluid mechanics and heat transfer within the porous matrix combustor. In the present calculations, porosities are 0.4 in first region of porous burner and in second region of porous region 0.87. For all simulations combustion is at atmospheric pressure. This

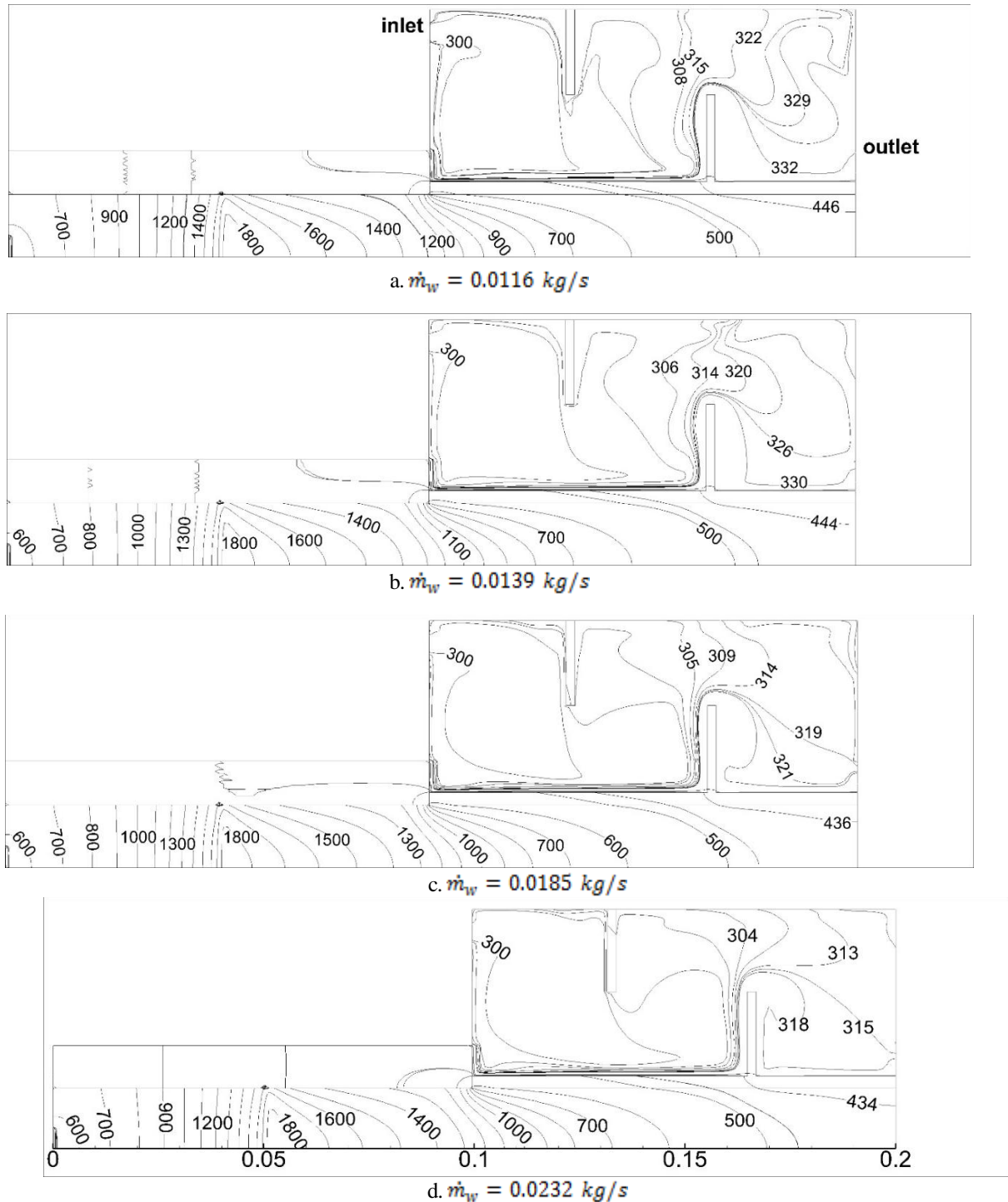


Figure 2. Isotherms (in Kelvin) for EAC=1.10 for different water mass flow rates (5 kW thermal power)

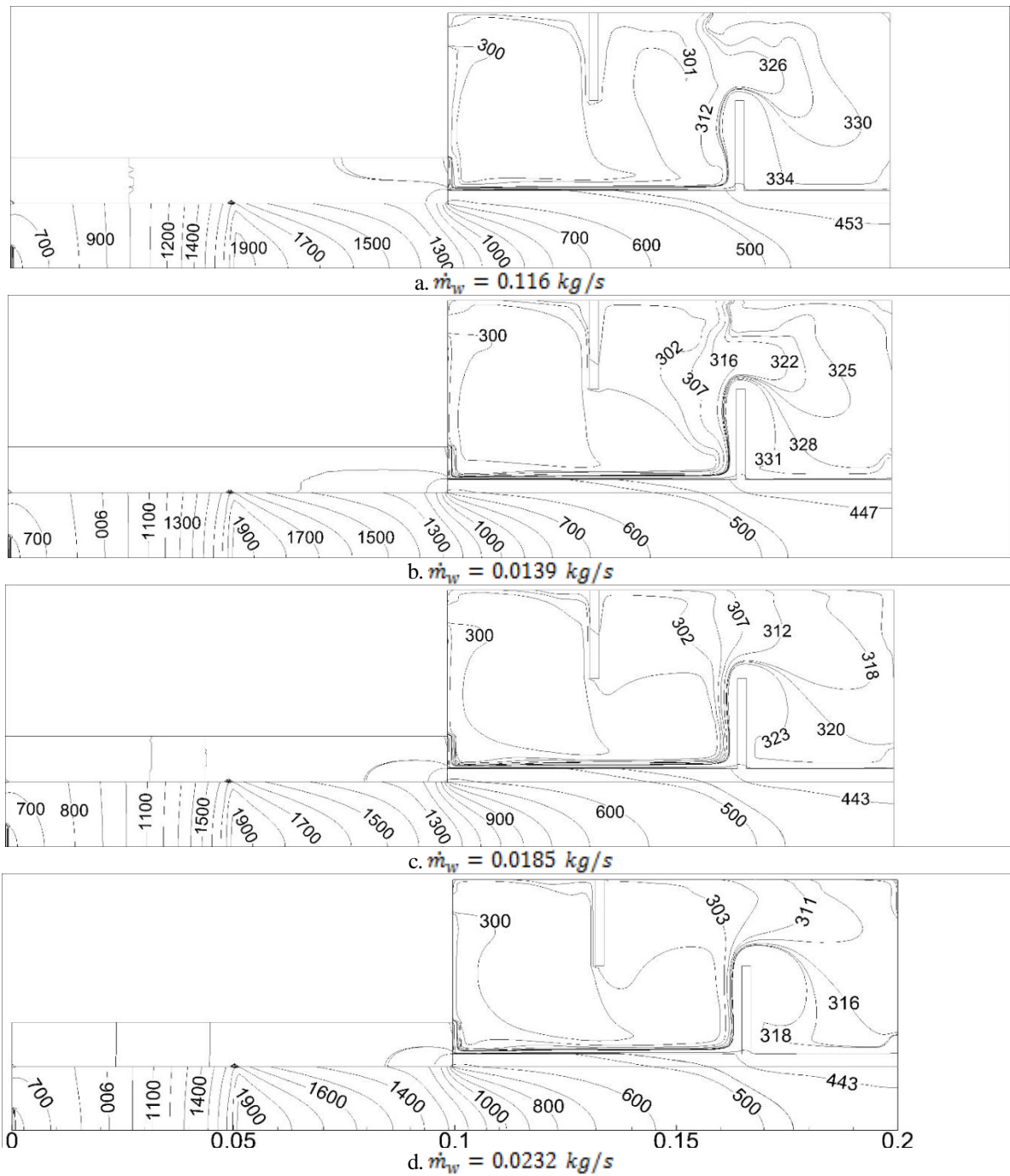


Figure 3. Isotherms (in Kelvin) for EAC=1.25 for different water mass flow rates (5 kW thermal power)

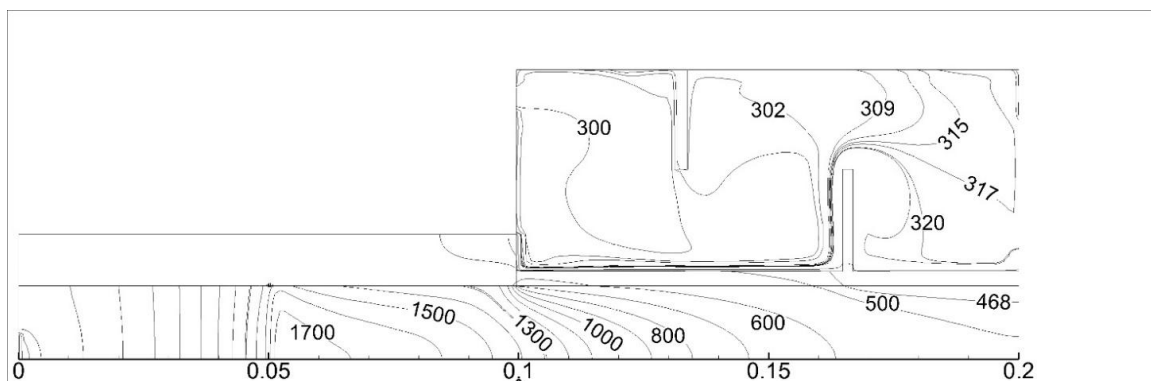


Figure 4. Isotherms (in Kelvin) for EAC=1.50, $\dot{m}_w = 0.0232 \text{ kg/s}$ (5 kW thermal Power)

investigation is mainly concerned with the effect of the inlet air/fuel gas velocity on the combustion efficiency/heat transfer efficacy of porous burner/heat exchanger assembly at a thermal power rating of 5 kW. Thermal power is based on the lower heating value of methane fuel. Results are presented for different inlet gas velocity, excess air coefficient and water mass flow rates for the heat exchanger.

Figures 2 through 4 show the isotherms for excess air coefficients of 1.10, 1.25 and 1.50, respectively. In general, the behavior of the temperature field within porous region is almost similar for all simulations with the same excess air coefficient and when the value of excess air coefficient increases, the maximum temperature within the porous burner decreases, as expected. As seen from Fig. 3 and 4, when the inlet velocity to the water tank increases, the average temperature within the water tank decreases.

In Fig. 5 major species concentrations are shown near the vicinity of the flame front. Note that reaction begins near $x=0.05$ m position, and this position is indeed the interface between high and low porosity regions. Species concentrations after the flame front are all very close to their equilibrium values, this indicates complete combustion. As opposed to a laminar freely propagating flame situation wherein the flame is a thin front with a thickness only a fraction of a millimeter, in this case the flame front is considerably thicker. This can be attributed to the nature of flame stabilization mechanism within the pores of the porous medium. This spread in the flame front might be speculated to be the cause of lower emission indices attributed to porous media combustion as the reaction occurs slowly and in a

more distributed fashion. Also note that quite similar behavior is observed in terms of species molefraction trends versus the flame coordinate.

Temperature and velocity distribution at the centerline of the porous burner for a variety of excess air ratios are plotted in Fig.6. This figure illustrates the effects of increasing the excess air ratio on the flame front position and the flame temperature and velocity on the centerline of the porous burner. As can be seen here, increasing the excess air ratio from 1.1 to 1.5 changes the flame front to the downstream and decrease the flame maximum temperature.

Fig. 6 demonstrates numerical results in comparison with experimental data obtained by Durst and Trimis (1996). At the first ignition point, the present results for excess air ratio 1.5 match very well with experimental data from Durst and Trimis (1996). The proposed porous burner as seen Fig. 1 is designed different style from available porous burner. For this reason, the axial temperature values are decreased to the end of porous burner because porous is cooled from outer surface by removing heat to the water tank and so the temperature difference between our prediction and experimental data of Durst and Trimis (1996) is occurred. The maximum combustion temperature, average exit temperature and efficiency of combustion are shown in Table 1. The maximum temperature is decreased as the excess air ratio is increased. The total efficient of all burner system is very satisfactory as seen in Table 1. Consequently, the porous material in the upstream region is better cooled, and it causes the flame front to move downstream and peak temperature to decrease.

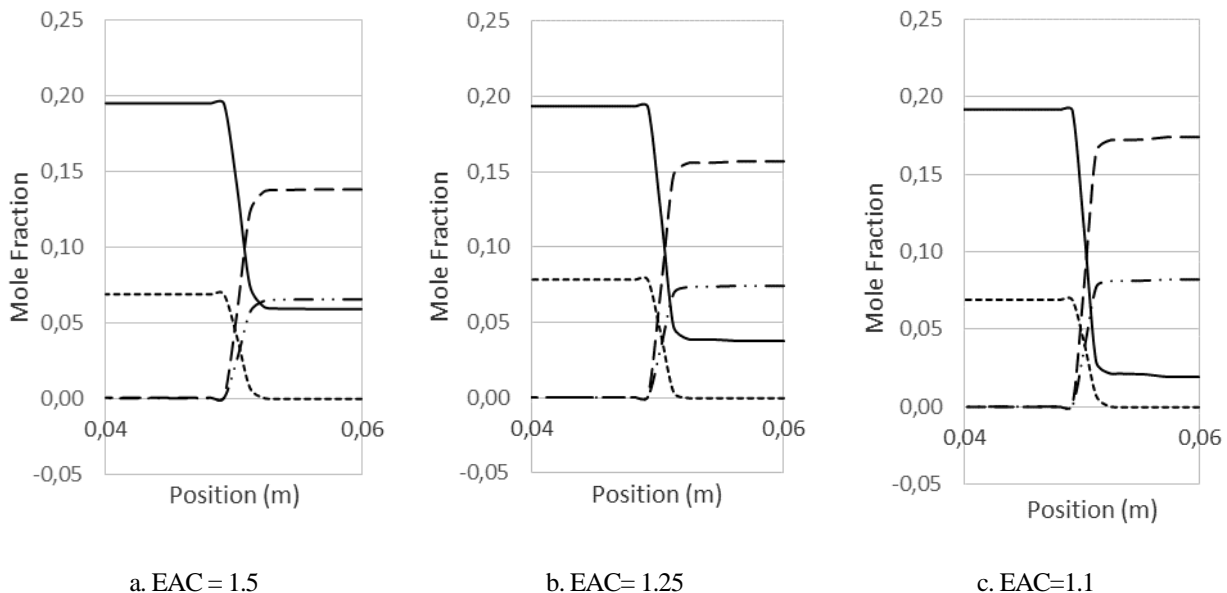


Figure 5. Centerline species mole fractions near the flame front for a number of excess air ratios

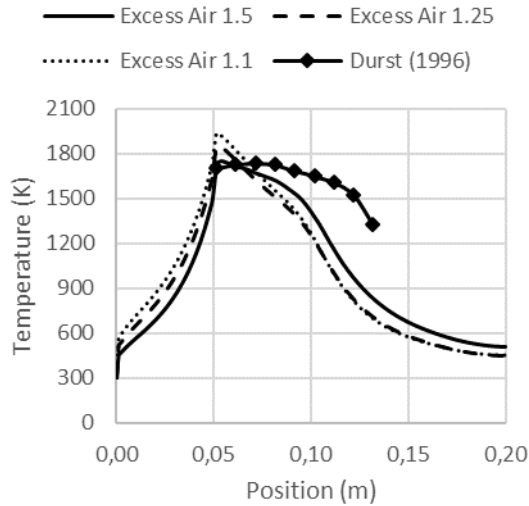


Figure 6. Temperature distribution at the symmetry axis

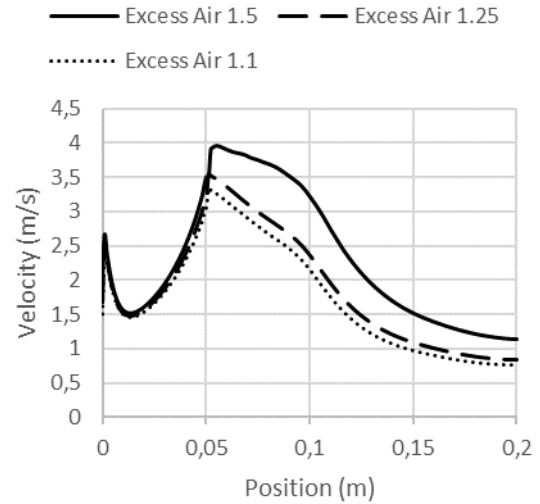


Figure 7. Velocity distribution at the symmetry axis

Table 2. Maximum combustion temperature, average water exit temperature and efficiencies

Excess Air Coefficient	Water Flow g/s	Maximum Temperature (K)	Water Outlet Temperature (K)	Combustion Efficiency	Heat Transfer Efficacy	Total Efficacy
1.5	23.2	1751.0	322.1	0.978	0.922	0.911
	11.6	1859.5	340.7	0.977	0.907	0.887
1.25	13.9	1860.7	334.2	0.976	0.901	0.879
	18.5	1854.5	325.1	0.978	0.900	0.880
	23.2	1853.2	320.6	0.975	0.928	0.905
1.1	11.6	1937.6	343.5	0.971	0.966	0.938
	13.9	1937.2	334.1	0.972	0.869	0.845
	18.5	1937.3	326.1	0.975	0.922	0.899
	23.2	1939.0	320.1	0.972	0.888	0.863

CONCLUSION

In this numerical study, reacting flow within a 5 kW power porous burner with integrated heat exchanger is solved numerically. Combustion chamber consists of two different porous regions and a premixing chamber additionally. Porous burner has two water tanks attached to remove heat through the combustor wall. The wall between the porous zone and water tank is assumed to have similar thermal properties, specific heat and thermal conductivity as steel. The fluid flow is assumed to be incompressible and two-dimensional and axisymmetric. The material of porous media is assumed to be a homogenous, isotropic and inert with negligible catalytic effects. In combustion modeling two step global methane-air oxidation mechanism that consists of two reactions and six chemical species.

While investigating the temperature distribution in porous burner, we mainly altered two variables; excess air ratio and water flow velocity. Water flow velocity, in the range of our study, did not show any considerable effect on both porous zones. On the other hand, excess air coefficient is clearly seen to be inversely proportional to maximum temperature in porous burner.

For all simulations, almost 90 percent of the heat released from the combustion is transferred to the water. Neither of the two variables mentioned above showed a significant effect on CO₂-CO combustion efficiency or heat transfer efficacy.

Combustion front in porous media is more distributed in comparison to freely propagating flames. This can account for lower thermal NO_x emissions (via the Zeldovich pathway), since the porous matrix effectively removes heat from the flame front and distributes it via conduction.

Furthermore, porous media combustion can also be deemed safer and more reliable especially for indoor applications. Only drawback of the porous media combustion is the increased pressure drop due to porous matrix yet this issue is not a major consideration for heating applications.

Future studies shall focus on coupling a flamelet combustion model for reacting flow within porous media in order to better understand further details of combustion (e.g. pollutant formation). Also three dimensional simulations are planned and comparisons shall be made with an experimental test rig.

ACKNOWLEDGEMENT

Authors gratefully acknowledge the support received from Turkish Scientific and Technical Research Council (TÜBİTAK) under contract no 114M672. We also acknowledge anonymous reviewers who helped us in improving this paper.

REFERENCES

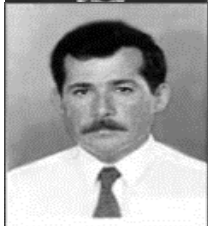
- Ata Y., Experimental investigation of a porous burner [In Turkish], Graduation Thesis, Istanbul Technical University Faculty of Aeronautics and Astronautics, 2010.
- Babkin, V.S., Korzhavin, A. A., Bunev, V. A., Propagation of premixed gaseous explosion flames in porous media, *Combustion and Flame*, 87, pp. 182-190, 1991.
- Barra A.J., Ellzey J.L., Heat re-circulation and heat transfer in porous burners, *Combustion and Flame*, 137, pp. 230–241, 2004.
- Baytaş A.C., Pop I., Free convection in a square porous cavity using a thermal non-equilibrium model, *International Journal of Thermal Science*, 141, pp. 861-870, 2002.
- Brenner G., Pickena K., Trimis D., Wawrzinek K., Weber T., Numerical and experimental investigation of matrix-stabilized methane/air combustion in porous inert media, *Combustion and Flame*, 123, pp. 201–213, 2000.
- Durst F., Trimis D., Compact porous medium burner and heat exchanger for household applications, European Commission project report (Contract No: JOE3-CT95-0019), 1996.
- Emonts B., Catalytic radiant burner for stationary and mobile applications, *Catalysis Today*, 47, 407-414, 1999.
- Henriquez-Vargas, L., Valeria, M., Bubnovich, V., Numerical study of lean combustibility limits extension in a reciprocal flow porous media burner for ethanol/air mixtures, *International Journal of Heat and Mass Transfer*, 89, pp. 1155-1163, 2015
- Iral, L., Amell, A., Performance study of an induced air porous radiant burner for household applications at high altitude, *Applied Thermal Engineering*, 83, pp. 31-39, 2015.
- Moraga, N. O., Rosas, C.E., Bubnovich, V. I., Solari N.A., On predicting two dimensional heat transfer in a cylindrical porous media combustor., *International Journal of Heat and Mass Transfer*, 51, pp 302- 311, 2008
- Shin, Y., Kim, Y., Numerical modeling for flame dynamics and combustion processes in a two-sectional porous burner with a detailed chemistry, *Journal of Mechanical Science and Technology*, 28 (11), pp. 4797-4805, 2014.
- Pantangi V.K., Mishra S.C., Muthukumar P., Reddy R., Studies on porous radiant burners for LPG cooking applications, *Energy*, 36, pp. 6074-6080, 2011.
- Patankar S., Numerical Heat Transfer and Fluid Flow, Hemisphere, New York, 1980.
- Smucker M.S., Ellzey J.L., Computational and experimental study of a two-section porous burner, *Combust. Sci. and Tech.*, 176, pp. 1171-1189, 2004.
- Takeo T, Sato K, Hase K., A theoretical study on an excess enthalpy flame, Proceedings of the 18th Symposium (International) on Combustion, Waterloo, pp. 465–72, 1981.
- Trimis, D., Stabilized combustion in porous media—applications of the porous burner technology in energy and heat engineering, AIAA Fluid 2000 Conference and Exhibition. Denver, CO, pp. 19-22 June, 2000.
- Yu, B., Kum, S.M., Lee, C.E., Lee, S., Combustion characteristics and thermal efficiency for premixed porous-media types of burners, *Energy*, pp. 1-8, 201.



TANJU ERGEN was born in Tekirdağ in 1989. He graduated from Tekirdağ Teacher Training High School in 2007. He received his BS degree in both aeronautical and aerospace engineering from Istanbul Technical University in 2013. Currently he is a research assistant at İstanbul Technical University Department of Aeronautical Engineering.



ONUR TUNÇER was born in İzmir in 1979. He graduated from İzmir Science Branch High School in 1997. In 2001 he received his BS degree in mechanical engineering from Middle East Technical University. He obtained his PhD degree in the same field from Louisiana State University in 2006. He started working at Istanbul Technical University Currently he is an associate professor at the Department of Aeronautical Engineering.



A. CİHAT BAYTAŞ was born in Ankara in 1954. In 1981, he received his BS degree in mechanical engineering from Yıldız Technical University and his MS in nuclear engineering from Boğaziçi University. He obtained his PhD degree in the same field from Istanbul Technical University. Currently he is a full professor at the Department of Aeronautical Engineering of Istanbul Technical University.